Article

Discovery Medicine 2023; 35(176): 405–417
https://doi.org/10.24976/Discov.Med.202335176.41

Development of FAP-Targeted Chimeric Antigen Receptor NK-92 Cells for Non-Small Cell Lung Cancer

Yang Fang[1], Yan-jing Wang[1], Hong-li Zhao[1], Xin Huang[1], Yi-nan Fang[1], Wen-yi Chen[1], Ruo-zhen Han[2], Ai Zhao[3,*], Ji-min Gao[1,4,*]

[1]Key Laboratory of Laboratory Medicine, Ministry of Education, School of Laboratory Medicine and Life Science, Wenzhou Medical University, 325005 Wenzhou, Zhejiang, China
[2]Radiotherapy Center, Wenzhou Central Hospital, 325000 Wenzhou, Zhejiang, China
[3]Department of Geriatrics, Affiliated Hangzhou First People's Hospital, Zhejiang University School of Medicine, 310006 Hangzhou, Zhejiang, China
[4]Zhejiang Qixin Biotech, 325036 Wenzhou, Zhejiang, China
*Correspondence: zhaoai618@126.com (Ai Zhao); jimingao@wmu.edu.cn (Ji-min Gao)
Published: 2 June 2023

Objectives: Over the past two decades, great progress has been made in advancing the early detection and multimodal treatment of non-small cell lung cancer (NSCLC). However, overall cure rates and survival rates of NSCLC are still not satisfactory, and research into new therapies is needed. This study attempted to construct human Fibroblast Activation Protein-Chimeric Antigen Receptor Natural killer (NK)-92 cells (hFAP-CAR-NK-92 cells) and explore their potential therapeutic effects in NSCLC.
Methods: Immunohistochemistry analysis was carried out to examine fibroblast activation protein (FAP) and Gasdermin E (GSDME) expression in clinical specimens of lung adenocarcinoma and squamous cell carcinoma tissue. Then the engineered hFAP-CAR-NK-92 cells efficiency was determined *in vitro* with lactate dehydrogenase (LDH) cytotoxicity assay and the cell morphology of A549, H226, and cancer-related fibroblast (CAF) was observed by electron microscopy. After the co-culture of target cells and effect cells, flow cytometry was employed for examining the CD107a expression in the effect cells, and western blotting was conducted for the cleavage levels of Caspase 3 and GSDME proteins in the target cells. The safety and efficacy of hFAP-CAR-NK-92 cells adoptive transfer immunotherapy in a tumor-bearing mouse were evaluated.
Results: Clinical studies have shown FAP positivity in patients with NSCLC. Compared with A549 or H226 cells alone, FAP expression was notably raised in A549+CAF cells or H226+CAF cells in nude mice, respectively ($p < 0.05$). The killing efficiency of K562 cells was not significantly different between hFAP-CAR-NK-92 and NK-92 cells ($p > 0.05$). The hFAP-CAR-NK-92 cells presented a higher killing efficiency against the hFAP-target (A549-hFAP, H226-hFAP and CAF-hFAP) cells than the NK-92 cells ($p < 0.05$). The degranulation of CD107a and cleavage levels of GSDME and Caspase 3 protein in the hFAP-CAR-NK-92 group were higher than those in the NK-92 group ($p < 0.05$). The 300 nM Granzyme B also induced pyroptosis in hFAP- or GSDME-positive cells ($p < 0.05$). *In vivo* experiments revealed that hFAP-CAR-NK-92 cells inhibited tumor progression of hFAP-positive NSCLC ($p < 0.05$).
Conclusions: In this study, we successfully constructed hFAP-CAR-NK-92 cells and confirmed that hFAP-CAR-NK-92 cells could target hFAP-positive NSCLC to inhibit the progression of NSCLC by activating the Caspase-3/GSDME pyroptosis pathway.

Keywords: fibroblast activation protein (FAP); non-small cell lung cancer (NSCLC); hFAP-CAR-NK-92 cells; caspase-3/GSDME; pyroptosis

Introduction

Non-small cell lung cancer (NSCLC), falling into malignant lung cancers, is the major contributor to cancer-related deaths worldwide [1]. A mandatory part of NSCLC management is molecular testing [2]. As a serine protease, fibroblast activation protein (FAP) is overexpressed in the fibroblasts associated with cancers and exerts important functions in a variety of malignant tumors' development and prognosis [3]. In addition, FAP expression can be observed in 90% of epithelial malignant tumors' stroma and some tumor cells but not in most normal tissues [4,5]. Highly expressed FAP-α in NSCLC has been shown in clinical studies to predict NSCLC patients' low survival [6]. Upregulated expression of FAP-α is likely to be correlated with inflammation and suppression of lymphocyte-dependent immune responses, leading to tumor progression [6,7]. Therefore, targeting FAP might be a potential therapeutic regimen for NSCLC.

Cancer-related fibroblasts (CAFs) expressing FAP have a correlation with poor prognosis and lower survival in breast, colorectal, pancreatic, and NSCLC [8]. High-density CAF-FAP$^+$ mesenchymal cells with highly infiltrated CD3 T cell and CD8 lymphocytes were associated

with better tumor prognosis, which might play an immune-aiding role in NSCLC [9]. Natural killer (NK) cells, belonging to cytotoxic lymphocytes, can identify and kill transformed cells without pre-sensitization. Moreover, the infiltration of NK cells into tumors reflects raised overall survival in tumor sufferers [10,11]. NK cells offer a first line of defense in their ability to link and coordinate innate and 'downstream' adaptive immune responses, making them an ideal platform for new cancer treatments [12]. Therefore, the application of FAP-targeting NK cells might be a new treatment for NSCLC.

NK cells may act as chimeric antigen receptor (CAR)-driven cytolysis' alternative cytotoxic effectors [13]. CAR-engineered NK cells, which can be obtained from allogeneic donors, represent a major advance in NK cell therapy [14]. CAR, a synthetic receptor known to promote the antitumor effect of T cells, was shown to respond significantly in some NSCLC patients combined with checkpoint-blocking therapy [15,16]. However, targeting specific antigens in NSCLC with engineered CAR-T cells was complex due to the shortage of tumor-specific antigens, immunosuppressive tumor microenvironment, low levels of CAR-T cell invasion into tumor tissue, and tumor antigen escape [17]. NK cells are known to be "serial killers" with NK and NK-92 cells (the cell line approved by the Food and Drug Administration as the first NK cell-based immunotherapy for clinical trials [18]) and one NK cell can kill up to 7–10 tumor cells [19,20]. Therefore, we hypothesized that the construction of FAP-targeting CAR-NK cells might contribute to the treatment of NSCLC.

Since NK cells only account for 10% of circulating lymphocytes approximately, selection/enrichment/expansion of NK cells by leukocyte isolation (from patients or donors) based on CD56 positive magnetic immunity and a feeder layer was time-consuming and costly [21–23]. Moreover, even if supplementing viral vectors, circulating NK cells still present unstable transfection efficiency (usually not very high) [24]. Despite the possibility of overcoming the difficulties of introducing CAR-coding genes into adequate circulating NK cells in some cases, NK-92 cells offer an open cellular platform for immunotherapy based on CAR [25,26]. In addition, in the presence of epidermal growth factor receptor (EGFR)-targeting monoclonal antibody cetuximab, NK-92-CD16 cells enhanced the cytotoxicity of tailored tyrosine kinase inhibitor (TKI)-resistant NSCLC cells [27]. Therefore, this study attempted to construct FAP-CAR-NK-92 cells and explore the intervention effect in NSCLC, to provide a theoretical basis for the treatment of NSCLC.

Materials and Methods

Clinical Subject Information and Sample Collection

Surgically resected tissues were taken from cancer patients (n = 10) who were hospitalized in Wenzhou Central Hospital, Wenzhou City, Zhejiang Province, China, from May 2020 to September 2022. Tissue sections were observed by HE staining and co-diagnosed as NSCLC with the assistance of 2 senior pathologists. The expression of FAP and Gasdermin E (GSDME) protein in tissues of NSCLC was analyzed by immunohistochemistry (IHC). Enrolled patients were staged according to UICC TNM Version 8 and classified in light of the pathology classification of lung cancer. The exclusion criteria were as follows: patients had received preoperative radiotherapy or chemotherapy and had been diagnosed with other malignancies within 5 years prior to diagnosis of NSCLC. This study has been approved by the Ethics Committee of Wenzhou Central Hospital (2022-132). All experiments in this study were performed based on the Declaration of Helsinki.

Construction of hFAP-CAR-NK-92 Cells

NK-92 cells (CL-0530, Procell) were cultured in the α Minimum Essential Medium (αMEM) + 0.2 mM inositol + 0.1 mM β-mercaptoethanol + 0.02 mM folic acid + 12.5% horse serum + 12.5% fetal bovine serum (FBS) + 100 μL/mL Interleukin (IL)-2 medium. To construct hFAP-CAR-NK-92 cells, logarithmic growing NK-92 cells were transfected with a pLenti-EF1α-anti-hFAP-CAR lentiviral expression vector (expressing second-generation CAR targeting human FAP, a multiplicity of infection [MOI] of 30). Signaling domains (41BB and CD3ζ) and an anti-FAP targeting moiety (scFv), CD8α hinge, and CD8 transmembrane domain (TM) constitute anti-FAP-CAR constructs [28]. The scFv was synthesized according to the anti-FAP antibody [29]. Stable hFAP-CAR expression in NK-92 cells was assessed using anti-mouse IgG (H+L), biotinylated antibody (#4410, Cell Signaling Technology, Danvers, MA, USA), then streptavidin-labelled phycoerythrin (PE) combined with APC-conjugated anti-CD56 antibody was supplemented for flow cytometry.

Cell Experiments and Treatments

Cell Lines

DMEM (Sigma-Aldrich, St. Louis, MO, USA) and 1640 medium (R8758, Sigma-Aldrich, St. Louis, MO, USA) containing 10% FBS + 1% penicillin and streptomycin was prepared for culturing A549 cells (iCell-h011, iCell) and H226 cells (iCell-h157, iCell), respectively. CAF cells were isolated from tumor tissues surgically removed from NSCLC patients. CAF cells were identified by hematoxylin and eosin (H&E) staining and flow cytometry (**Supplementary Fig. 1**). The culture of CAF cells was conducted in DMEM (Sigma-Aldrich, St. Louis, MO, USA) with 10% FBS + 1% non-essential amino acids + 1% penicillin and streptomycin. As for 293T cells (iCell-h237, iCell) and K562 (iCell-h118, iCell), DMEM (Sigma-Aldrich, St. Louis, MO, USA) containing 10% FBS + 1% penicillin and streptomycin was used for their culture. All cell samples were cultured at 37 °C and 5% CO_2. The cell

lines used passed STR certification and mycoplasma testing.

Then, A549-hFAP, H226-hFAP and CAF-hFAP cells were digested by 0.25% trypsin (Gibco, Los Angeles, CA, USA). The hFAP antigen fragment was cloned into a PiggyBac transposon plasmid synthesized by Hanhe Biological Company, and the expression of hFAP was constructed through seamless cloning, the cells were transfected with the PiggyBac Transposon system (System Biosciences, Palo Alto, CA, USA) was applied using Lipofectamine™ 2000 Transfection Reagent (Life Technologies, Gaithersburg, MD, USA) following the manufacturer's instructions. The FAP expression of A549-hFAP, H226-hFAP and CAF-hFAP cells was detected through flow cytometry.

Cytotoxicity Assays

A lactate dehydrogenase (LDH) release assay was constructed to determine the cytotoxicity of NK-92 cells or hFAP-CAR-NK-92 cells against A549-hFAP, H226-hFAP, CAF-hFAP cells and K562 cells. This assay was finished with the help of the LDH Cytotoxicity Assay Kit (Promega, Madison, WI, USA) following the manufacturer's protocol. Target cells (1×10^4) were seeded in 96-well flat-bottom plates for 12 h, and then NK-92 cells or hFAP-CAR-NK-92 were supplemented into each well at various effect/target ratios. After 6 h, LDH release assays were carried out. The formula for calculating specific lysis percentage was applied as follows: Cytotoxicity (%) = (experimental LDH release – spontaneous LDH release)/(maximal LDH release – spontaneous LDH release) $\times$ 100. The experimental conditions were all in triplicate, and all experiments were repeated 3 times.

Intracellular Delivery of Granzyme B

The GSDME fragment, which was provided by Hanhe Biotechnology Co., Ltd., was constructed in a PiggyBac transposon plasmid by seamless cloning. To construct 293T-GSDME cells and K562-GSDME cells, about 1×10^6–5×10^6 cells of 293T and K562 cells were electroporated with 2 μg transposase and 6 μg transposon DNA plasmid in an electroporator (Lonza Group Ltd., Basel, Switzerland) by using the corresponding Nucleofector® Kit [30]. In order to electroporate granzyme B into cells, 1.5×10^6 cells of A549 cells, 293T-GSDME cells, K562-GSDME cells and K562 cells were mixed with different concentrations of granzyme B (100 nM and 300 nM [Abnova, Taipei, Taiwan]) in 100 μL 4D-Nucleofector™ Solution, respectively. The cells were incubated in Nucleocuvettes™ for 5 min at room temperature and then they were electroporated using the Lonza 4D-Nucleofector™ System, according to the system program [31]. The cells were transferred to humidified conditions (37 °C and 5% CO_2) for 12 h incubation and follow-up analysis.

Animal Experiments

Female nude mice and NOD-SCID mice (age: 6 weeks; weight: 20–25 g) were acquired from Beijing Vital River Laboratory Animal Technology Co., Ltd. Nude mice were randomly divided into the A549 group (A549, 1.5×10^6 cells/mouse), A549+CAF group (A549:CAF, 1:2, 4.5×10^6 cells/mouse), H226 group (H226, 1.5×10^6 cells/mouse), and H226+CAF group (H226:CAF, 1:2, 4.5×10^6 cells/mouse), 3 mice/group. The 100 μL cell suspension with phosphate-buffered saline (PBS) was injected subcutaneously under the armpits of the mice. After the injection, the nude mice were kept in the animal house for 34 days. Caliper measurements were applied to measure tumor growth, and the formula of length $\times$ (width)^2 $\times$ 0.5 was applied to calculate tumor volumes. After mice were sacrificed by intravenous administration of sodium pentobarbital (40–60 mg/kg), the tumors were removed, fixed and examined.

The tumor formation of A549 cells+CAF cells and H226 cells+CAF cells in NOD-SCID mice were constructed as the above. Mice were grouped when the tumors were palpable. According to different weights, mice were allocated into 3 groups (n = 3) randomly. The mice in groups received one of the following caudal vein injections: (1) 100 μL PBS (Control group), (2) 5×10^6 irradiate NK-92 cells in 100 μL sterile PBS (NK-92 group), or (3) 5×10^6 irradiate parental NK-92 cells in 100 μL sterile PBS (hFAP-CAR-NK-92 group) [32]. The tumor volume was recorded as above, and treatment was applied on days 12, 19 and 26. On day 30, the mice were euthanized for sacrifice and the tumors were obtained for examination.

Hematoxylin-Eosin (HE) Staining

The fixed tissues were sequentially embedded and sliced. After 12-h baking at 60 °C, the slices were dewaxed to water with xylene and gradient ethanol. Hematoxylin and eosin were used for tissue staining. The slices were dehydrated, sealed, and then observed under a microscope (Olympus, Tokyo, Japan).

Immunohistochemistry (IHC)

Slices were dewaxed to water for antigen's thermal repair. The endogenous enzymes in slices were inactivated for 10 min by 1% periodate acid at room temperature. Slices were dropped with suitably diluted primary anti-FAP (1:200, #66562, Cell Signaling Technology, Danvers, MA, USA), anti-GSDME (1:200, ab230482, Abcam, Cambridge, UK), anti-CD56 (1:200, #99746, Cell Signaling Technology, Danvers, MA, USA) and anti-Ki-67 (1:200, ab92742, Abcam, Cambridge, UK) at 4 °C. On the next day, 50–100 μL anti-IgG antibody was added into the slices for 30 min of incubation at 37 °C. After slice sealing, the DAB working solution was used for observation under a microscope (Olympus).

Flow Cytometry

FAP-CAR expression in NK-92 cells was assessed via biotinylated antibody (#9417, Cell Signaling Technology, Danvers, MA, USA) and anti-mouse IgG (H+L), then added with streptavidin-labelled PE combined with APC-conjugated anti-CD56 antibody (#73521, #51997, Cell Signaling Technology, Danvers, MA, USA). PE-labelled anti-human FAP antibody (#427819, Bio-techne, Minneapolis, MN, USA) was adopted to verify the FAP expression on target tumor cells and CAFs. Degranulation response in NK-92 cells and hFAP-CAR NK-92 cells was appraised with APC-conjugated anti-CD107a Antibody (#508921, Bio-techne, Minneapolis, MN, USA). Data were acquired and analyzed by CytExpert (Beckman Coulter, Miami, FL, USA).

Electron Microscope Observation

Cells were immobilized in 2.5% glutaraldehyde and 1% osmium (18456, TED PELLA INC) for 6~12 h and 1~2 h, respectively. The cells were dehydrated by gradient ethanol (30–100%) and propylene oxide (M25514, Meryer, Shanghai, China). Subsequently, the cells were immersed in epoxy propane: epoxy resin (1:1) and pure epoxy resin for embedding, respectively. Then, it was baked in an oven for 60 h. After taking out the embedded block and repairing the block, the ultra-thin section was carried out, and the copper net was retrieved. Sections were electronically stained (lead, uranium). Finally, transmission electron microscopy (7700, Hitachi, Tokyo, Japan) was utilized to observe the treated sections and a digital camera (ER-B, AMT) to record images.

Western Blotting

The extraction of total protein from cells was performed through Radio Immunoprecipitation Assay (RIPA) protein extraction reagent (ThermoFisher Scientific, Waltham, MA, USA). A bicinchoninic acid (BCA) protein quantification kit was utilized for determining protein concentration. Next, the isolation of 200 μg protein samples was implemented through 12% sodium dodecyl sulfate-polyacrylamide gel electrophoresis (SDS-PAGE). After the isolated proteins were transferred onto the polyvinylidene fluoride membrane, the membrane was activated by methanol, sealed with 5% skim milk, and then incubated with the primary antibodies overnight. The primary antibodies used included anti-Caspase 3 (1:1000, #9662, Cell Signaling Technology, Danvers, MA, USA), anti-GSDME (1:1000, ab215191, Abcam, Cambridge, UK), anti-N-GSDME (1:1000, ab222408, Abcam, Cambridge, UK), anti-β-actin (1:1000, ab179467, Abcam, Cambridge, UK). The membrane was then incubated with secondary anti-IgG (1:1000, ab133470, Abcam, Cambridge, UK). Visualization was performed for analysis.

Data Statistics and Analysis

Graphpad Prism8.0 statistical software (Version X; La Jolla, CA, USA) was employed to statistically analyze the data in this study. The measurement data were displayed as mean $\pm$ standard deviation (*SD*). Normality and homogeneity of variance tests were carried out first, which satisfied homogeneity of variance and normal distribution. Student's *t*-test was used for comparisons between two groups, and a one-way Analysis of Variance (ANOVA) for comparisons among multiple groups. $p < 0.05$ suggested a significant difference.

Results

FAP Expression was Involved in the Tumor Formation of NSCLC

To explore FAP expression and clinicopathological characteristics, we summarized the included patients' clinical information in this article (Table 1). H&E and immunohistochemical analysis showed that NSCLC patients were FAP positive in tumor cells or fibroblasts and tumor cells (Table 1, Fig. 1A,B and **Supplementary Fig. 2**). The positive rates of FAP in lung adenocarcinoma and squamous cell carcinoma were 42.2% (35 patients) and 48.9% (22 patients), respectively (Table 1, Fig. 1C). In nude mice, the tumor volume of the A549+CAF cells group increased significantly in contrast to the A549 cells group ($p < 0.05$) (Fig. 1D). Relative to the H226 cells group, tumor volumes of the H226+CAF cells group climbed up notably ($p < 0.05$) (Fig. 1D). IHC analysis exhibited that FAP expression was markedly upregulated in the A549+CAF cells group in comparison with the A549 cells group ($p < 0.05$) (Fig. 1E). In addition, FAP expression significantly increased in the H226+CAF cells group relative to the H226 cells group ($p < 0.05$) (Fig. 1F). In a nutshell, FAP expression participated in the NSCLC development, and targeting FAP might inhibit NSCLC progression.

Construction and Functional Validation of hFAP-CAR-NK-92 Cells

We further constructed the recombinant lentivirus expression vector hFAP-CAR and transfected it in NK-92 cells (Fig. 2A). After transfection of NK-92 cells with a retroviral vector encoding the hFAP-CAR, the hFAP-CAR-NK-92 cells expressing hFAP-CAR were obtained by culture of monoclonal cells (Fig. 2B). To investigate the changes of cell-killing function after CAR modification, NK-92 cells and hFAP-CAR-NK-92 cells were co-incubated with K562 cells by 1:1, 5:1 and 10:1, respectively (Fig. 2C). The outcomes indicated no statistical differences in cell-killing efficiency ($p > 0.05$) (Fig. 2C). We then constructed A549-hFAP cells, H226-hFAP cells and CAF-hFAP cells. Flow cytometry presented that the FAP expression rate in A549-hFAP cells, H226-hFAP cells and CAF-hFAP cells were 80.62%, 86.45% and 75.63%, significantly

Table 1. Expression and clinicopathological analysis of FAP in lung adenocarcinoma and lung squamous cell carcinoma.

Characteristics	Number (128%)	Tissue types		χ^2	*p*-value
		LUAD	LUSC		
		(83 %)	(45 %)		
Sex				6.476	0.011
Male	41 (32.0)	33 (39.8)	8 (17.8)		
Female	87 (68.0)	50 (60.2)	37 (82.2)		
Age				2.231	0.135
<65	54 (42.2)	39 (47.0)	15 (33.3)		
≥65	74 (57.8)	44 (53.0)	30 (66.7)		
Differentiation				12.257	< 0.001
Medium-high	61 (47.7)	49 (59.0)	12 (26.7)		
Low	67 (52.3)	34 (41.0)	33 (73.3)		
LNM				24.798	< 0.001
N1+N2	70 (54.7)	32 (38.6)	38 (84.4)		
No	58 (45.3)	51 (61.4)	7 (15.6)		
Clinical stages				0.469	0.791
I	65 (50.8)	43 (51.8)	22 (48.9)		
II	25 (19.5)	17 (20.5)	8 (17.8)		
III	38 (29.7)	23 (27.7)	15 (33.3)		
FAP				0.533	0.465
Low	71 (55.5)	48 (57.8)	23 (51.1)		
High	57 (44.5)	35 (42.2)	22 (48.9)		

Note: LUSC, lung squamous cell carcinoma; LUAD, lung adenocarcinoma; LNM, lymph node metastasis.

higher than that in A549 cells, H226 cells and CAF cells ($p < 0.05$) (Fig. 2D). The killing efficiency of hFAP-CAR-NK-92 cells against A549-hFAP cells, H226-hFAP cells and CAF-hFAP cells were much higher in comparison with NK-92 cells *in vitro* ($p < 0.05$) (Fig. 2E). CD107a expression in hFAP-CAR-NK-92 cells was significantly higher in the A549-hFAP, H226-hFAP and CAF-hFAP groups ($p < 0.05$), but no changes were shown in the K562 group compared with that in NK-92 cells ($p > 0.05$) (Fig. 2F,G). The above results proved that FAP-positive cells could be targeted and killed by hFAP-CAR-NK-92 cells.

hFAP-CAR-NK-92 Cells Induced Pyroptosis of Target Cells

Cell morphology observation showed that the A549-hFAP, H226-hFAP and CAF-hFAP cells in the NK-92 group appeared as round swelling and some organelles degenerated (Fig. 3A). The A549-hFAP, H226-hFAP and CAF-hFAP cells in the hFAP-CAR-NK-92 group were swollen, the structure of some organelles such as mitochondria was damaged, the cell membrane was incomplete with gaps or contents overflowing, indicating pyroptosis (Fig. 3A). Protein assay showed GSDME was expressed in A549 cells, H226 cells and CAF cells (CAF1 and CAF2) ($p < 0.05$), but it was not expressed in 293T cells, NK-92 cells and K562 cells ($p > 0.05$) (Fig. 3B). IHC assay showed highly expressed GSDME in lung adenocarcinoma compared with lung squamous cell carcinoma tissues ($p < 0.05$) (Fig. 3C). Besides, the cleavage levels of Caspase 3 and GSDME in the hFAP-CAR-NK-92 group were higher than those in the NK-92 group, and the cleavage levels of GSDME and Caspase 3 in the A549-hFAP, H226-hFAP and CAF-hFAP cells were equivalent to others ($p < 0.05$) (Fig. 3D). All in all, hFAP-CAR-NK-92 cells mediated pyroptosis of FAP-positive target cells.

Granzyme B-GSDME Pathway Induced Pyroptosis in Target Cells Expressing GSDME

Cell morphology observation showed that compared with the granzyme B (100 nM) group, the A549-hFAP, H226-hFAP and 293T-GSDME cells in the granzyme B (300 nM) group appeared pyroptosis, with cells swollen, the structure of organelles (such as mitochondria) was damaged and the cell membrane was incomplete with gaps or contents overflowing (Fig. 4A). The western blot assay showed the GSDME overexpression of 293T and K562 cells (Fig. 4B). In K562 cells, GSDME's cleavage levels were not expressed, and the cleavage levels of Caspase 3 were higher in the granzyme B (300 nM) group than those in the granzyme B (0 nM) group ($p < 0.05$) (Fig. 4C). Furthermore, the cleavage levels of GSDME and Caspase 3 in the granzyme B (300 nM) group were higher than those in the granzyme B (0 nM) group ($p < 0.05$), and the cleavage levels of GSDME and Caspase 3 in the A549-hFAP, H226-hFAP, 293T-GSDME and K562-GSDME cells were equivalent to one another (Fig. 4D). These results suggested

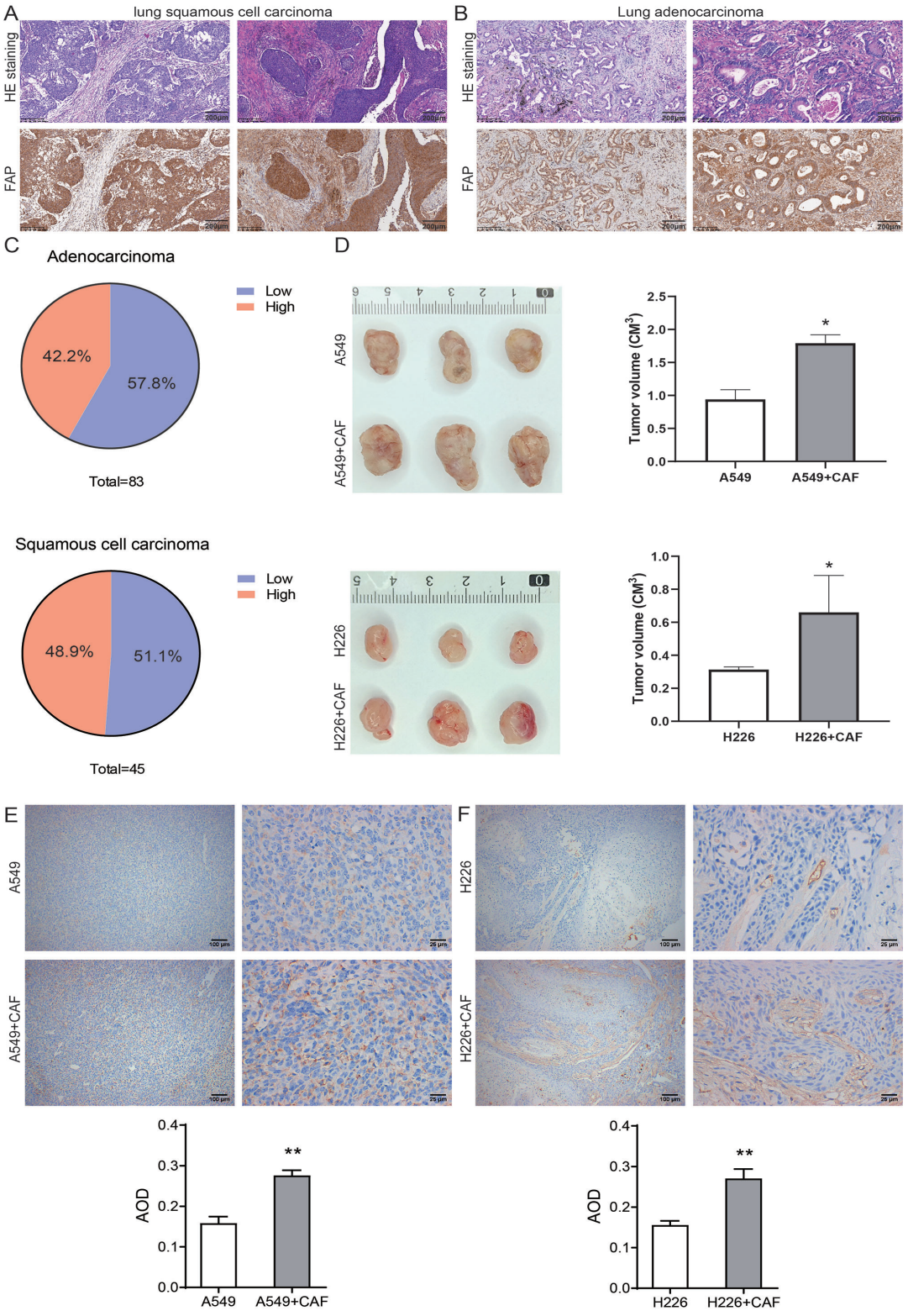

Fig. 1. FAP expression in tumor formation of NSCLC. (A,B) The expression of FAP in (A) lung squamous cell carcinoma and (B) adenocarcinoma tissues were analyzed by HE staining (upper panels) (200 μm) and IHC staining (lower panels) (Scale bar = 200 μm) (n = 3). (C) The ratio of FAP positives in lung adenocarcinoma and squamous cell carcinoma. High stands for high FAP expression and Low stands for low FAP expression. (D) Tumor pattern and volume analysis of A549 or H226 cells alone and A549 or H226 cells mixed with CAF cells (n = 3). (E,F) FAP expression was tested through IHC (Scale bar = 100 and 25 μm) (n = 3). *$p < 0.05$, **$p < 0.01$ *vs.* A549 or H226 group.

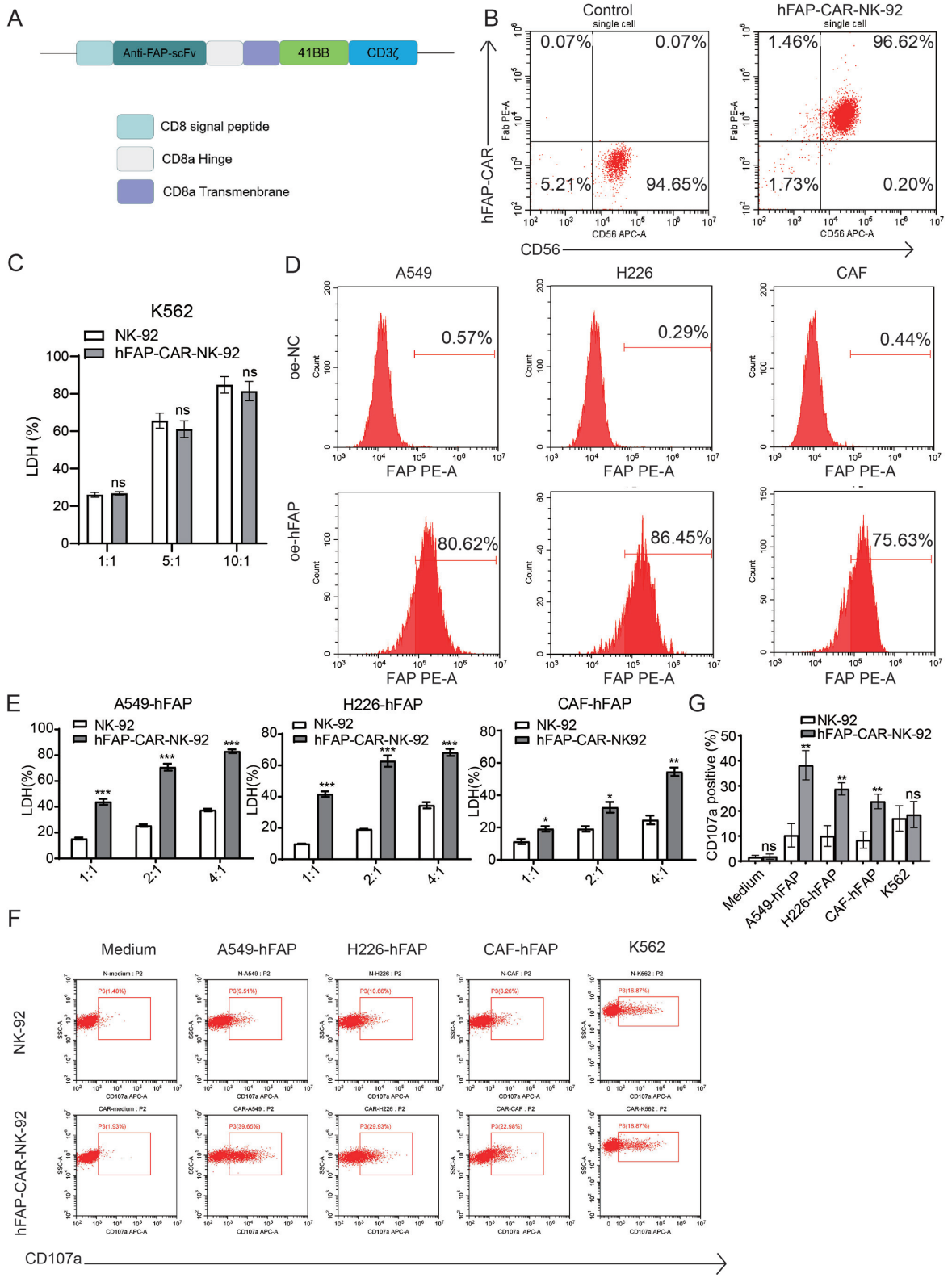

Fig. 2. Construction of hFAP-CAR-NK-92 cells and identification of their killing function *in vitro*. (A) Diagram illustration of hFAP-CAR in lentiviral vector. (B) Flow cytometry analyzed the positive rate of hFAP-CAR in hFAP-CAR-NK-92 cells (n = 3). (C) Cell cytotoxicity was measured by the LDH assay (n = 3). (D) Flow cytometry to test the expression rate of FAP in A549, H226 and CAF cells (n = 3). (E) Cell cytotoxicity was determined with the LDH assay (n = 3). (F,G) Flow cytometry and statistical analysis of CD107a expression (n = 3). *$p < 0.05$, **$p < 0.01$ or ***$p < 0.001$ *vs* NK-92 group. ns, no significance.

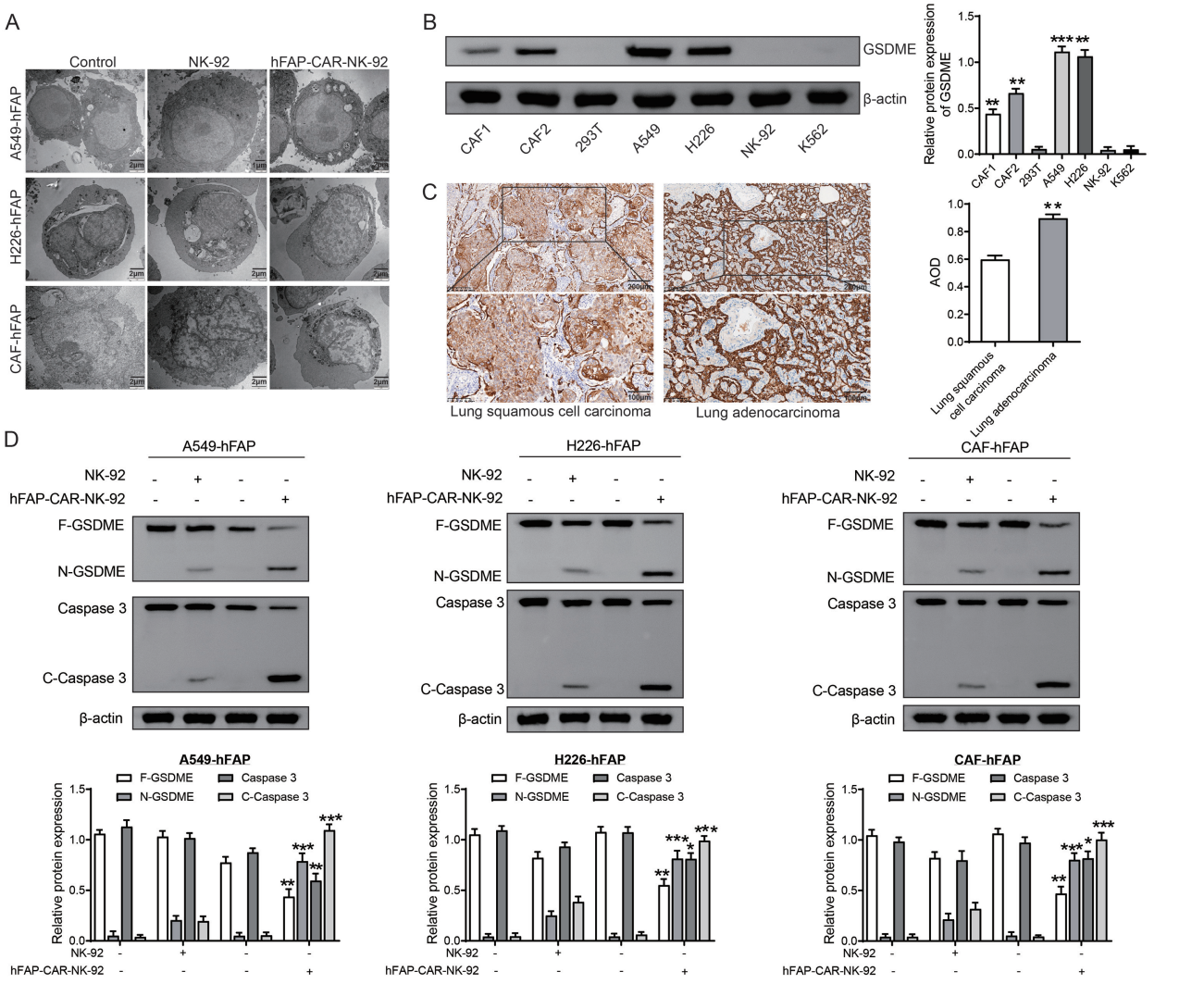

Fig. 3. hFAP-CAR-NK-92 cells-induced pyroptosis of target cells. (A) The morphology of A549-hFAP, H226-hFAP and CAF-hFAP cells were observed by electron microscopy (2 μm) (n = 1). (B) The detection of GSDME expression by western blot (n = 3). (C) The GSDME expression in lung squamous cell carcinoma and lung adenocarcinoma tissues was detected by IHC (Scale bar = 200 and 100 μm) (n = 3). (D) Western blot to check the cleavage of Caspase 3 and GSDME proteins in A549-hFAP, H226-hFAP and CAF-hFAP cells. C-Caspase 3 represented cleaved-Caspase 3. N-GSDME represented cleaved-GSDME (n = 3). *$p < 0.05$, **$p < 0.01$ or ***$p < 0.001$ *vs* NK-92 or lung squamous cell carcinoma tissues group.

that pyroptosis occurred through the granzyme B-GSDME pathway.

Stronger Effect of hFAP-CAR-NK-92 Cells than NK-92 Cells in Inhibiting Tumor Growth in Vivo

Tumorigenesis in Non-obese diabetic-server combined immune-deficiency (NOD-SCID) mice was used to estimate the efficacy and safety of hFAP-CAR-NK-92 cell therapy (Fig. 5A). Compared with the NK-92 cell group, the tumor volume was significantly reduced in the NOD-SCID mice with the hFAP-CAR-NK-92 cell group ($p < 0.05$) (Fig. 5B). Additionally, Ki-67 expression declined significantly while CD56 expression raised notably in the NOD-SCID mice with the hFAP-CAR-NK-92 cells relative to the NK-92 cell group ($p < 0.05$) (Fig. 5C). All above findings proved that the hFAP-CAR-NK-92 cells suppressed tumor growth more effectively than the NK-92 cells.

Discussion

FAP+CAFs have attracted much attention in the field of clinical diagnosis and treatment of cancer [33]. Upregulation of FAP was associated with poorer clinical outcomes in most cancer types, but the biological mechanisms behind these clinical observations remain unclear [34]. CAFs, discovered in epithelial neoplasm stroma and featured by FAP overexpression, can be used in cancer imaging and therapy [3,35,36]. Our clinical study found FAP positiv-

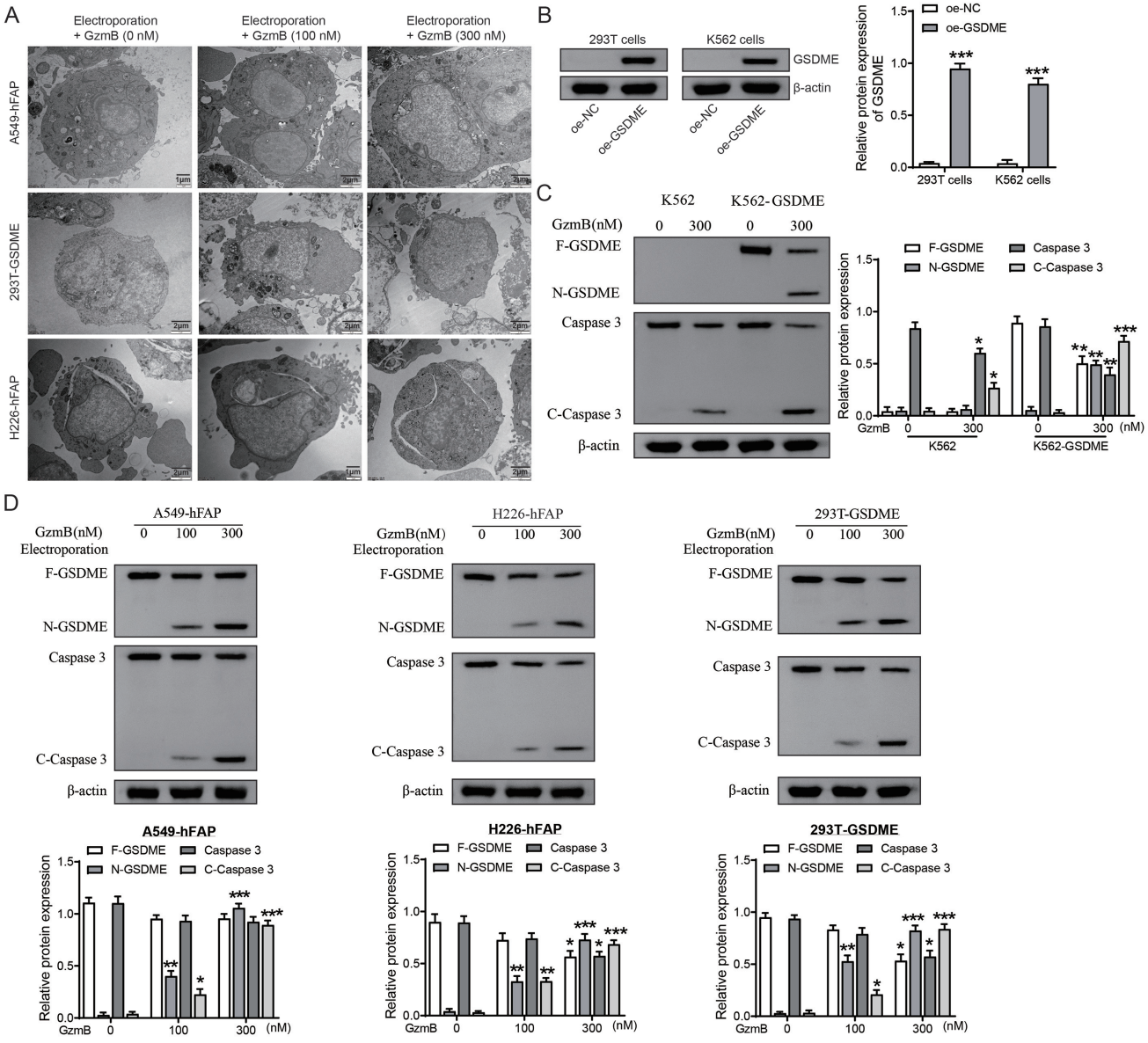

Fig. 4. Granzyme B-GSDME pathway-induced pyroptosis in target cells expressing GSDME. (A) The morphology of A549-hFAP, H226-hFAP and 293T-GSDME cells were observed by electron microscopy (Scale bar = 1 μm and 2 μm) (n = 1). (B) The GSDME expression was examined via western blot (n = 3). (C,D) Western blot to determine the cleavage of Caspase 3 and GSDME proteins in K562, K562-GSDME, A549-hFAP, H226-hFAP and 293T-GSDME cells (n = 3). GzmB represented Granzyme B; C-Caspase 3 represented cleaved-Caspase 3. N-GSDME represented cleaved-GSDME. *$p < 0.05$, **$p < 0.01$ or ***$p < 0.001$ *vs* oe-NC or GzmB (0 nM) group.

ity in NSCLC patients, which might be a treatment target. In addition, human lung CAFs enhanced the protection of A549 and H1299 cells in Transwell® and direct co-culture and promoted the radioresistance of lung cancer cells [37]. Animal experiments revealed that, compared with A549 or H226 cells, FAP expression was upregulated in the co-culture of A549+CAF cells or H226+CAF cells in tumorigenesis. These studies suggested that FAP was involved in the development of NSCLC and might be a potential therapeutic target.

The interaction between NK cells and CAFs constitutes a related but relatively poorly studied crosstalk relationship in the tumor microenvironment (TME) [38]. Currently, NK-92 cells are prone to be scaled to clinical stages under good manufacturing practice states, and their safety has been demonstrated in some phase I clinical research [39]. The combination of NK-92MICD64 cells and mAb (targeting TROP2 and FAP) methods was twice as cytotoxic as NK-92MICD4 cells at a 20:1 effector-to-target cell ratio [40]. At a good safety threshold, Delta-like ligand 3 (DLL3)–CAR-NK-92 cells induced tumor regression in

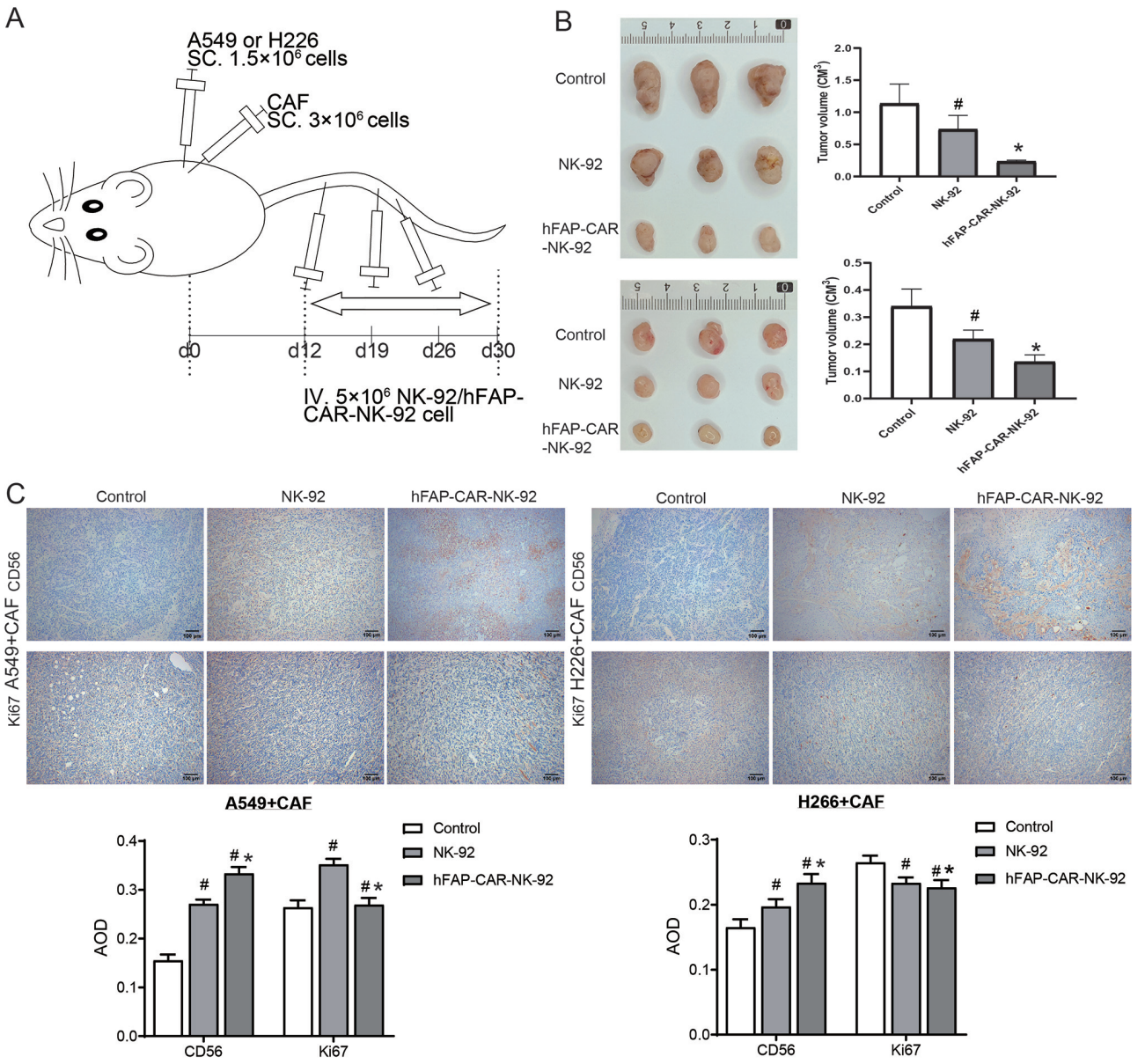

Fig. 5. hFAP-CAR-NK-92 cell therapy inhibited tumor growth in NOD-SCID mice. (A) The schematic of tumor models and cell therapy. (B) Tumor morphology and volume were observed and analyzed (n = 3). (C) The expression of CD56 and Ki-67 in tumor tissue was analyzed by IHC (Scale bar = 100 and 25 μm) (n = 3). $^{\#}p < 0.05$ *vs* Control group; $^{*}p < 0.05$ *vs* NK-92 group.

an H446-derived lung metastatic tumor model [41]. In our study, no differences were observed in K562 cells' killing efficiency between NK-92 and hFAP-CAR-NK-92 cells. While the hFAP-CAR-NK-92 cells had a higher killing efficiency against hFAP-target (A549-hFAP, H226-hFAP and CAF-hFAP) cells than NK-92 cells. These studies have proved that hFAP-CAR-NK-92 cells could effectively play a targeted killing function, but the specific mechanism and clinical safety of hFAP-CAR-NK-92 cells need to be evaluated.

The Caspase-3/GSDME pathway switches in cancer cells between apoptosis and pyroptosis [42]. Cisplatin promotes secondary necrosis by inducing Caspase-3 activation and GSDME-NT production in A549 cells [43]. Caspase-3 specifically cleaves GSDME in its linker to form a GSDME-N fragment that penetrates the cell membrane, thereby inducing pyroptosis [44]. CAR-T cells release granzyme B to make Caspase 3 activated rapidly in target cells, which cleaves GSDME, leading to extensive pyroptosis [45]. Apart from exhibiting specific cytotoxicity *in vitro*, EpCAM-CAR-NK-92 also was known to specifically identify EpCAM-positive colorectal cancer cells and set free cytokines, such as granzyme B, perforin and Interferon (IFN)-γ [46]. By directly cleaving GSDME at a similar location to Caspase 3, killer cell granzyme B also functions in activating target cells' Caspase-independent pyroptosis

[47]. Our study also confirmed that GSDME and Caspase 3 protein cleavage levels in A549-hFAP and H226-hFAP cells treated with hFAP-CAR-NK-92 cells were higher than those treated with NK-92 cells. Moreover, hFAP-CAR-NK-92 cells induced pyroptosis of hFAP target cells, which was similar to the treatment of 300 nM granzyme B. These findings suggested that hFAP-CAR-NK-92 cells could be targeted to induce pyroptosis of FAP+ cancer cells through Caspase-3/GSDME activation and hFAP-CAR-NK-92 cells might be used in clinical immunotherapy.

CAR-NK cells present a higher safety profile than CAR-T cells, particularly in averting side effects like cytokine release syndrome [48]. Anti-MSLN-CAR-NK cells remarkably eliminated gastric cancer cells in peritoneal and subcutaneous tumor models and notably extended the survival time of intraperitoneal tumor-bearing mice [49]. By virtue of CAR-NK-92 cells targeting organoids expressing Epidermal growth factor receptor variant III (EGFRvIII), tumor antigen-specific cytotoxicity was proved by related research [50]. *In vivo*, we confirmed that hFAP-CAR-NK-92 cells inhibited the progression of A549 or H226+CAF cells with safety and no side effects.

Conclusions

To sum up, hFAP-CAR-NK-92 cells were successfully established in our study. Moreover, we have revealed that hFAP-CAR-NK-92 inhibits tumor progression through activation of the Caspase-3/GSDME pyroptosis pathway in hFAP-positive NSCLC, which provides new insights into the development of clinical cellular immunotherapy for NSCLC.

Availability of Data and Materials

The data used to support the findings of this study are available from the corresponding author upon request.

Author Contributions

YF, AZ and JMG designed the research study. YF, AZ and JMG performed the research. YJW, HLZ, XH, YNF, WYC and RZH provided help and advice on the experiments. YJW, HLZ, XH, YNF, WYC and RZH analyzed the data. All authors contributed to editorial changes in the manuscript. All authors read and approved the final manuscript. All authors have participated sufficiently in the work and agreed to be accountable for all aspects of the work.

Ethics Approval and Consent to Participate

This study has been approved by the Ethics Committee of Wenzhou Central Hospital (2022-132). All experiments in this study were performed based on the Declaration of Helsinki. All mice experiments were carried out according to the applicable guidelines and regulations approved by the approved by Institution Animal Care and Use Committee (IACUC), Zhejiang Experimental Animal Center (Approval No. ZJCLA-IACUC-20050025). All subjects signed the consent form before participation in the study.

Acknowledgment

We thank technicians from the core facilities (School of Laboratory Medicine and Life Science, Wenzhou Medical University) for assistance in FACS and image analysis.

Funding

This study was supported by the Scientific Research Fund of National Health Commission of China (WKJ-ZJ-1928 by Jimin Gao), Wenzhou Municipal Science and Technology Research Program (ZS2017014, 2018ZY001 by Jimin Gao), Construction Fund of Key Medical Disciplines of Hangzhou (No. OO20200055 by Ai Zhao), and Shandong Provincial Key R&D programs (2021CXGC011102 by Jimin Gao).

Conflict of Interest

Dr. Ji-min Gao is an employee of Zhejiang Qixin Biotech. The authors declare no conflict of interest.

Supplementary Material

Supplementary material associated with this article can be found, in the online version, at https://doi.org/10.24976/Discov.Med.202335176.41.

References

[1] Thai AA, Solomon BJ, Sequist LV, Gainor JF, Heist RS. Lung cancer. Lancet (London, England). 2021; 398: 535–554.

[2] Imyanitov EN, Iyevleva AG, Levchenko EV. Molecular testing and targeted therapy for non-small cell lung cancer: Current status and perspectives. Critical Reviews in Oncology/Hematology. 2021; 157: 103194.

[3] Lindner T, Altmann A, Giesel F, Kratochwil C, Kleist C, Krämer S, *et al*. ^{18}F-labeled tracers targeting fibroblast activation protein. EJNMMI Radiopharmacy and Chemistry. 2021; 6: 26.

[4] Liu R, Li H, Liu L, Yu J, Ren X. Fibroblast activation protein: A potential therapeutic target in cancer. Cancer Biology & Therapy. 2012; 13: 123–129.

[5] Tlsty TD. Stromal cells can contribute oncogenic signals. Seminars in Cancer Biology. 2001; 11: 97–104.

[6] Liao Y, Ni Y, He R, Liu W, Du J. Clinical implications of fibroblast activation protein-α in non-small cell lung cancer after curative resection: a new predictor for prognosis. Journal of Cancer Research and Clinical Oncology. 2013; 139: 1523–1528.

[7] Nam Y, Choi CM, Park YS, Jung H, Hwang HS, Lee JC, *et al*. CDCP1 Expression Is a Potential Biomarker of Poor Prognosis in Resected Stage I Non-Small-Cell Lung Cancer. Journal of Clinical Medicine. 2022; 11: 341.

[8] Mathieson L, O'Connor RA, Stewart H, Shaw P, Dhaliwal K,

Williams GOS, *et al*. Fibroblast Activation Protein Specific Optical Imaging in Non-Small Cell Lung Cancer. Frontiers in Oncology. 2022; 12: 834350.

[9] Kilvaer TK, Rakaee M, Hellevik T, Østman A, Strell C, Bremnes RM, *et al*. Tissue analyses reveal a potential immune-adjuvant function of FAP-1 positive fibroblasts in non-small cell lung cancer. PLoS ONE. 2018; 13: e0192157.

[10] Michel T, Ollert M, Zimmer J. A Hot Topic: Cancer Immunotherapy and Natural Killer Cells. International Journal of Molecular Sciences. 2022; 23: 797.

[11] Vlachostergios PJ, Karathanasis A, Tzortzis V. Expression of Fibroblast Activation Protein Is Enriched in Neuroendocrine Prostate Cancer and Predicts Worse Survival. Genes. 2022; 13: 135.

[12] Pockley AG, Vaupel P, Multhoff G. NK cell-based therapeutics for lung cancer. Expert Opinion on Biological Therapy. 2020; 20: 23–33.

[13] Stankovic B, Bjørhovde HAK, Skarshaug R, Aamodt H, Frafjord A, Müller E, *et al*. Immune Cell Composition in Human Non-small Cell Lung Cancer. Frontiers in Immunology. 2019; 9: 3101.

[14] Sivori S, Pende D, Quatrini L, Pietra G, Della Chiesa M, Vacca P, *et al*. NK cells and ILCs in tumor immunotherapy. Molecular Aspects of Medicine. 2021; 80: 100870.

[15] Zeltsman M, Dozier J, McGee E, Ngai D, Adusumilli PS. CAR T-cell therapy for lung cancer and malignant pleural mesothelioma. Translational Research: the Journal of Laboratory and Clinical Medicine. 2017; 187: 1–10.

[16] Hu Z, Zheng X, Jiao D, Zhou Y, Sun R, Wang B, *et al*. LunX-CAR T Cells as a Targeted Therapy for Non-Small Cell Lung Cancer. Molecular Therapy Oncolytics. 2020; 17: 361–370.

[17] Qu J, Mei Q, Chen L, Zhou J. Chimeric antigen receptor (CAR)-T-cell therapy in non-small-cell lung cancer (NSCLC): current status and future perspectives. Cancer Immunology, Immunotherapy: CII. 2021; 70: 619–631.

[18] Pan K, Farrukh H, Chittepu VCSR, Xu H, Pan CX, Zhu Z. CAR race to cancer immunotherapy: from CAR T, CAR NK to CAR macrophage therapy. Journal of Experimental & Clinical Cancer Research: CR. 2022; 41: 119.

[19] Papak I, Chruściel E, Dziubek K, Kurkowiak M, Urban-Wójciuk Z, Marjański T, *et al*. What Inhibits Natural Killers' Performance in Tumour. International Journal of Molecular Sciences. 2022; 23: 7030.

[20] Bhat R, Watzl C. Serial killing of tumor cells by human natural killer cells–enhancement by therapeutic antibodies. PloS one. 2007; 2: e326.

[21] Min B, Choi H, Her JH, Jung MY, Kim HJ, Jung MY, *et al*. Optimization of Large-Scale Expansion and Cryopreservation of Human Natural Killer Cells for Anti-Tumor Therapy. Immune Network. 2018; 18: e31.

[22] Fujisaki H, Kakuda H, Shimasaki N, Imai C, Ma J, Lockey T, *et al*. Expansion of highly cytotoxic human natural killer cells for cancer cell therapy. Cancer Research. 2009; 69: 4010–4017.

[23] Klingemann H. Are natural killer cells superior CAR drivers? Oncoimmunology. 2014; 3: e28147.

[24] Boissel L, Betancur M, Wels WS, Tuncer H, Klingemann H. Transfection with mRNA for CD19 specific chimeric antigen receptor restores NK cell mediated killing of CLL cells. Leukemia Research. 2009; 33: 1255–1259.

[25] Uherek C, Tonn T, Uherek B, Becker S, Schnierle B, Klingemann HG, *et al*. Retargeting of natural killer-cell cytolytic activity to ErbB2-expressing cancer cells results in efficient and selective tumor cell destruction. Blood. 2002; 100: 1265–1273.

[26] Boissel L, Betancur-Boissel M, Lu W, Krause DS, Van Etten RA, Wels WS, *et al*. Retargeting NK-92 cells by means of CD19- and CD20-specific chimeric antigen receptors compares favorably with antibody-dependent cellular cytotoxicity. Oncoimmunology. 2013; 2: e26527.

[27] Park HR, Ahn YO, Kim TM, Kim S, Kim S, Lee YS, *et al*. NK92-CD16 cells are cytotoxic to non-small cell lung cancer cell lines that have acquired resistance to tyrosine kinase inhibitors. Cytotherapy. 2019; 21: 603–611.

[28] Bughda R, Dimou P, D'Souza RR, Klampatsa A. Fibroblast Activation Protein (FAP)-Targeted CAR-T Cells: Launching an Attack on Tumor Stroma. ImmunoTargets and Therapy. 2021; 10: 313–323.

[29] Pfizenmaier Klaus, Wajant Harald, Moosmayer Dieter, Wueest Thomas. Site-specific, antibody-mediated activation of proapoptotic cytokine: Amaice (antibody-mediated apoptosis inducing cytokine). World Intellectual Property Organization. WO2001EP10364. 07 Sep 2001.

[30] DeWitt MA, Corn JE, Carroll D. Genome editing via delivery of Cas9 ribonucleoprotein. Methods (San Diego, Calif.). 2017; 121-122: 9–15.

[31] Zhou Z, He H, Wang K, Shi X, Wang Y, Su Y, *et al*. Granzyme A from cytotoxic lymphocytes cleaves GSDMB to trigger pyroptosis in target cells. Science (New York, N.Y.). 2020; 368: eaaz7548.

[32] Navarrete-Galvan L, Guglielmo M, Cruz Amaya J, Smith-Gagen J, Lombardi VC, Merica R, *et al*. Optimizing NK-92 serial killers: gamma irradiation, CD95/Fas-ligation, and NK or LAK attack limit cytotoxic efficacy. Journal of Translational Medicine. 2022; 20: 151.

[33] Lindner T, Giesel FL, Kratochwil C, Serfling SE. Radioligands Targeting Fibroblast Activation Protein (FAP). Cancers. 2021; 13: 5744.

[34] Fitzgerald AA, Weiner LM. The role of fibroblast activation protein in health and malignancy. Cancer Metastasis Reviews. 2020; 39: 783–803.

[35] Toms J, Kogler J, Maschauer S, Daniel C, Schmidkonz C, Kuwert T, *et al*. Targeting Fibroblast Activation Protein: Radiosynthesis and Preclinical Evaluation of an ^{18}F-Labeled FAP Inhibitor. Journal of Nuclear Medicine: Official Publication, Society of Nuclear Medicine. 2020; 61: 1806–1813.

[36] Slania SL, Das D, Lisok A, Du Y, Jiang Z, Mease RC, *et al*. Imaging of Fibroblast Activation Protein in Cancer Xenografts Using Novel (4-Quinolinoyl)-glycyl-2-cyanopyrrolidine-Based Small Molecules. Journal of Medicinal Chemistry. 2021; 64: 4059–4070.

[37] Ji X, Ji J, Shan F, Zhang Y, Chen Y, Lu X. Cancer-associated fibroblasts from NSCLC promote the radioresistance in lung cancer cell lines. International Journal of Clinical and Experimental Medicine. 2015; 8: 7002–7008.

[38] Malchiodi ZX, Weiner LM. Understanding and Targeting Natural Killer Cell-Cancer-Associated Fibroblast Interactions in Pancreatic Ductal Adenocarcinoma. Cancers. 2021; 13: 405.

[39] Romanski A, Uherek C, Bug G, Seifried E, Klingemann H, Wels WS, *et al*. CD19-CAR engineered NK-92 cells are sufficient to overcome NK cell resistance in B-cell malignancies. Journal of Cellular and Molecular Medicine. 2016; 20: 1287–1294.

[40] Hintz HM, Snyder KM, Wu J, Hullsiek R, Dahlvang JD, Hart GT, *et al*. Simultaneous Engagement of Tumor and Stroma Targeting Antibodies by Engineered NK-92 Cells Expressing CD64 Controls Prostate Cancer Growth. Cancer Immunology Research. 2021; 9: 1270–1282.

[41] Liu M, Huang W, Guo Y, Zhou Y, Zhi C, Chen J, *et al*. CAR NK-92 cells targeting DLL3 kill effectively small cell lung cancer cells *in vitro* and *in vivo*. Journal of Leukocyte Biology. 2022; 112: 901–911.

[42] Jiang M, Qi L, Li L, Li Y. The caspase-3/GSDME signal pathway as a switch between apoptosis and pyroptosis in cancer. Cell Death Discovery. 2020; 6: 112.

[43] Zhang CC, Li CG, Wang YF, Xu LH, He XH, Zeng QZ, *et al*. Chemotherapeutic paclitaxel and cisplatin differentially induce pyroptosis in A549 lung cancer cells via caspase-3/GSDME activation. Apoptosis: an International Journal on Programmed Cell Death. 2019; 24: 312–325.

[44] Wang Y, Gao W, Shi X, Ding J, Liu W, He H, *et al*. Chemotherapy drugs induce pyroptosis through caspase-3 cleavage of a gasdermin. Nature. 2017; 547: 99–103.

[45] Liu Y, Fang Y, Chen X, Wang Z, Liang X, Zhang T, *et al*. Gasdermin E-mediated target cell pyroptosis by CAR T cells triggers cytokine release syndrome. Science Immunology. 2020; 5: eaax7969.

[46] Zhang Q, Zhang H, Ding J, Liu H, Li H, Li H, *et al*. Combination Therapy with EpCAM-CAR-NK-92 Cells and Regorafenib against Human Colorectal Cancer Models. Journal of Immunology Research. 2018; 2018: 4263520.

[47] Zhang Z, Zhang Y, Xia S, Kong Q, Li S, Liu X, *et al*. Gasdermin E suppresses tumour growth by activating anti-tumour immunity. Nature. 2020; 579: 415–420.

[48] Tang X, Yang L, Li Z, Nalin AP, Dai H, Xu T, *et al*. First-in-man clinical trial of CAR NK-92 cells: safety test of CD33-CAR NK-92 cells in patients with relapsed and refractory acute myeloid leukemia. American Journal of Cancer Research. 2018; 8: 1083–1089.

[49] Cao B, Liu M, Huang J, Zhou J, Li J, Lian H, *et al*. Development of mesothelin-specific CAR NK-92 cells for the treatment of gastric cancer. International Journal of Biological Sciences. 2021; 17: 3850–3861.

[50] Schnalzger TE, de Groot MH, Zhang C, Mosa MH, Michels BE, Röder J, *et al*. 3D model for CAR-mediated cytotoxicity using patient-derived colorectal cancer organoids. The EMBO Journal. 2019; 38: e100928.